

9-2019

Water entry impact dynamics of diving birds

Saburel I. Sharker
Utah State University

Sean Holekamp
Naval Undersea Warfare Center, Newport, RI

Mohammad M. Mansoor
Utah State University

Tadd T. Truscott
Utah State University

Follow this and additional works at: https://digitalcommons.wcupa.edu/bio_facpub



Part of the [Biomechanics Commons](#)

Recommended Citation

Sharker, S. I., Holekamp, S., Mansoor, M. M., & Truscott, T. T. (2019). Water entry impact dynamics of diving birds. *Bioinspiration & Biomimetics*, 14(5), 1-12. <http://dx.doi.org/10.1088/1748-3190/ab38cc>

This Article is brought to you for free and open access by the Biology at Digital Commons @ West Chester University. It has been accepted for inclusion in Biology Faculty Publications by an authorized administrator of Digital Commons @ West Chester University. For more information, please contact wcressler@wcupa.edu.

PAPER

Water entry impact dynamics of diving birds

To cite this article: Saberul I Sharker *et al* 2019 *Bioinspir. Biomim.* **14** 056013

View the [article online](#) for updates and enhancements.



IOP | ebooks™

Bringing you innovative digital publishing with leading voices to create your essential collection of books in STEM research.

Start exploring the collection - download the first chapter of every title for free.

Bioinspiration & Biomimetics



PAPER

Water entry impact dynamics of diving birds

RECEIVED
23 March 2019

REVISED
1 August 2019

ACCEPTED FOR PUBLICATION
6 August 2019

PUBLISHED
29 August 2019

Saberul I Sharker¹, Sean Holekamp², Mohammad M Mansoor¹, Frank E Fish³ and Tadd T Truscott¹

¹ Department of Mechanical and Aerospace Engineering, Utah State University, Logan, UT, United States of America

² Naval Undersea Warfare Center, Newport, RI, United States of America

³ Department of Biology, West Chester University, West Chester, PA, United States of America

E-mail: taddtruscott@gmail.com

Keywords: impact dynamics, beak angle, diving birds, jerk, accelerometer

Supplementary material for this article is available [online](#)

Abstract

Some seabirds (such as northern gannets and brown boobies) can dive from heights as high as 30 m reaching speeds of up to 24 m s^{-1} as they impact the water surface. The physical geometry of plunge diving birds, particularly of the beak, allows them to limit high impact forces compared to non-diving birds. Numerically simulated data for one species (northern gannet) provides some insight into the impact forces experienced during diving, however, no reliable experimental data with real bird geometries exist for comparison purposes. This study utilizes eleven 3D printed diving bird models of three types of birds: plunge-diving (five), surface-diving (five) and dipper (one), with embedded accelerometers to measure water-entry impact accelerations for impact velocities ranging between $4.4\text{--}23.2 \text{ m s}^{-1}$. Impact forces for all bird types are found to be comparable under similar impact conditions and well within the safe zone characterized by neck strength as found in recent studies. However, the time that each bird requires to reach maximum impact acceleration from impact is different based on its beak and head shape and so is its effect, represented here by its derivative (i.e. jerk). We show that surface diving birds have high non-dimensional jerk, which exceed a safe limit estimated from human impact analysis, whereas those by plunge divers do not.

1. Introduction

The beaks of diving birds are adapted to forage in the aquatic environment. Many of these birds feed mostly on fish, catching their prey mainly in two different ways: surface diving and plunge diving. Birds like the common loon and the double-crested cormorant rest on the surface of the water and then dive when they target their prey, and are hence called surface divers. Surface divers also include the common eider, which dive to feed on benthic invertebrates, predominately sessile blue mussels (Guillemette *et al* 1992). On the other hand, specialized plunge divers such as the northern gannet and the brown booby dive from heights as high as 30 m reaching speeds of 24 m s^{-1} as they impact the water (Ropert-Coudert *et al* 2004) while folding their wings to minimize the impact force and conserve momentum (Lee and Reddish 1981, Brierley and Fernandes 2001). Plunge diving birds are able to dive 1.2 to 12.6 m in depth and a further 22 m by active flapping (Adams and Walter 1993, Le Corre 1997, Garthe *et al* 2000, Brierley and Fernandes 2001). These

birds follow two types of dive patterns: V-shaped and U-shaped. It has been found that whenever these birds want to go deeper, they perform U-shaped dives from higher heights, which are usually vertical-entry dives (Machovsky-Capuska *et al* 2011a). Although plunge diving is a highly successful technique for catching food, it does not always end with a hearty meal. Diving at these high speeds can sometimes be fatal as the birds can collide with one another (Machovsky-Capuska *et al* 2011b).

Some birds, like the herring gull, feed by dipping (Castro and Huber 2008), hence classified as dippers, and forage by scavenging or picking fish from the surface. In addition, Herring gulls are occasionally observed to make shallow plunge dives (Verbeek 1977, Sibly and McCleery 1983) but are not classified as plunging specialists. We include this species of birds as a representative between plunging and surface diving birds.

The negative accelerations associated with impact reported in limited studies on plunge diving birds appear contradictory. Numerical simulations performed by Wang *et al* (2013) found very large decel-

eration values at impact (23 times gravitational acceleration, g , for an impact velocity of 24 m s^{-1}) resulting in considerable water entry forces on the gannet body. On the other hand, experiments by Ropert-Coudert *et al* (2004) found zero to very small decelerations during the impact stage of water entry. They attached data loggers to the back of the neck and tail of northern gannets but the sampling frequency (32 Hz) may have been too low to detect the short duration impact event. Thus, higher sampling frequency experiments are required to accurately record the impact dynamics.

The neck is potentially the most vulnerable part of the bird especially when diving. Recent studies (Chang *et al* 2016) have revealed brown boobies and northern gannets may be well within the safe limits of neck failure during diving. Chang *et al* attached an elastic beam to a cone representing the bird neck and skull. The stiffness of the elastic beam was measured and compared to the neck stiffness of a dead bird. The cone-beam system was dropped into water and the bending forces were measured for impact velocities ranging from 0.5 to 2.5 m s^{-1} (max impact speeds of Brown boobies and northern gannets is approximately 24 m s^{-1}). An unstable and a stable region were identified and theoretical analogs from the empirical data indicated that these birds dive well within their safe neck bending limits. Unfortunately, there is a general lack of data for neck strength and head adaptations that correlate with plunge diving in the literature. Herein, we attempt to show how the beak shape can affect the deceleration of plunge divers up to speeds they experience in nature.

Among other factors that affect water-entry impact accelerations, the wing sweptback angle and water-entry inclination angle with relation to dropping heights have been studied by Liang *et al* for a fabricated bionic Gannet (Liang *et al* 2013). They found that the peak impact acceleration increases with increasing dropping height and water-entry angle, whereas the peak impact acceleration decreases with increasing wing sweptback angle. The differences between the peak impact accelerations obtained by them and by us for similar impact conditions are likely due to the differences in projectile masses between the two methods. In recent years, there has been a huge interest in the fabrication of unmanned vehicles that are capable of functioning both in air and under water. Yang *et al* (2015) classified the current partially-featured AquaUAV (Unmanned Air Vehicle) into three categories from the scope of the whole UAV field, namely, the seaplane UAV, the submarine-launched UAV, and the submersible UAV. Furthermore, some of the unmanned aquatic and air vehicles are made with fixed wings (Weisler *et al* 2017) and some others with folded wings for reduced drag during diving (Wu *et al* 2019).

The water impact of canonical shapes such as spheres and cones can be divided into a number of distinct phases (May 1975, Truscott *et al* 2014) and applied to the water entry of birds: 1. shock-wave phase (figure 3(A) frame 1), 2. flow-forming phase (frame 2),

3. open-cavity phase (frame 3), 4. closed-cavity phase (frame 6), 5. collapsing cavity phase (pinch-off, frame 7), and 6. fully-wetted phase (not shown). Experimental studies of projectiles (Moghisi and Squire 1981, Eroshin *et al* 1980, Shiffman and Spencer 1945, Bodily *et al* 2014) show that the forces of blunt body water entry can be maximum anywhere between phase 1 and 5. The forces of the initial stages of impact must be measured in order to make estimates of the dynamic strength for a given structure (Korobkin and Pukhnachov 1988).

This study focuses on the initial phases of impact for eleven 3D printed diving bird head models (five plunge divers, five surface divers and one dipper). These 3D printed bird head models are used to analyze the water-entry dynamics with embedded accelerometers to measure impact accelerations for vertical entry, as higher height dives are made vertically by the birds (Machovsky-Capuska *et al* 2011a). While it is realized that there might be other factors that affect the survivability of diving birds, studying the free-surface impact forces in relation to the bird's physical features gives insight into understanding the properties that enable plunge diving birds to dive underwater at high speeds but not surface diving birds.

2. Methods

2.1. Birds

Specimens of five plunge diving birds, five surface diving birds and one dipper were obtained from the Delaware Museum of Natural History. The typical properties of these species, including mass, length and dive height, as obtained in nature are presented in table 1 (collected from Alderfer (2008) and Perrins 2003). Heads of the birds were 3D scanned with the GoMeasure 3D HDI Advance R1 scanning system (Amherst, VA). All birds were adults with the feathers on the head unruffled. Birds were chosen from available specimens at the museum that were aquatic and in good condition. Representative species of plunge diving birds and surface diving birds were chosen for comparison. The birds were all positioned with the head and beak extended anteriorly, as in during plunge diving. Only the scanned heads and beaks were used to make the models, thus negating any effect of the body. The scans reflected an accurate model of live bird heads as the specimens included both the beak and the skull. The posterior parts of the scans were modified (using MeshLab and SolidWorks® software) to incorporate an internal accelerometer near the neck region (figures 1(B) and (C)) and the corresponding drawings were made to resemble the contour of real birds (figure 1(A)) as closely as possible. The birds were then 3D printed with the Dimension SST 1200es™ and treated with acetone to smooth out imperfections from 3D printing. The properties of the 3D printed bird head models are presented in table 2. The exact densities of the specific birds used in this paper are difficult

Table 1. List of birds used and their typical properties.

Bird type	Name of bird	Mass (kg)	Length (cm)	Typical dive height (m)
Plunge diving birds				
1	Belted kingfisher (<i>Megaceryle alcyon</i>)	0.14 to 0.17	28 to 35	10 to 12
2	Brown booby (<i>Sula leucogaster</i>)	1.00 to 1.80	64 to 85	15 to 20
3	Common tern (<i>Sterna hirundo</i>)	0.10 to 0.20	31 to 38	1 to 6
4	Northern gannet (<i>Morus bassanus</i>)	2.20 to 3.60	81 to 110	10 to 30
5	Red-footed booby (<i>Sula sula</i>)	0.85 to 1.10	69 to 79	10 to 30
Dipper				
1	Herring gull (<i>Larus argentatus</i>)	0.80 to 1.25	56 to 66	1 to 12
Surface diving birds				
1	Atlantic puffin (<i>Fratercula arctica</i>)	0.40 to 0.65	28 to 30	0
2	Common eider (<i>Somateria mollissima</i>)	1.92 to 2.21	50 to 71	0
3	Double crested cormorant (<i>Phalacrocorax auritus</i>)	1.20 to 2.50	70 to 90	0
4	Common loon (<i>Gavia immer</i>)	2.50 to 6.0	66 to 91	0
5	Red-breasted merganser (<i>Mergus serrator</i>)	0.80 to 1.35	51 to 64	0

Data has been collected from Alderfer (2008) and Perrins (2003).

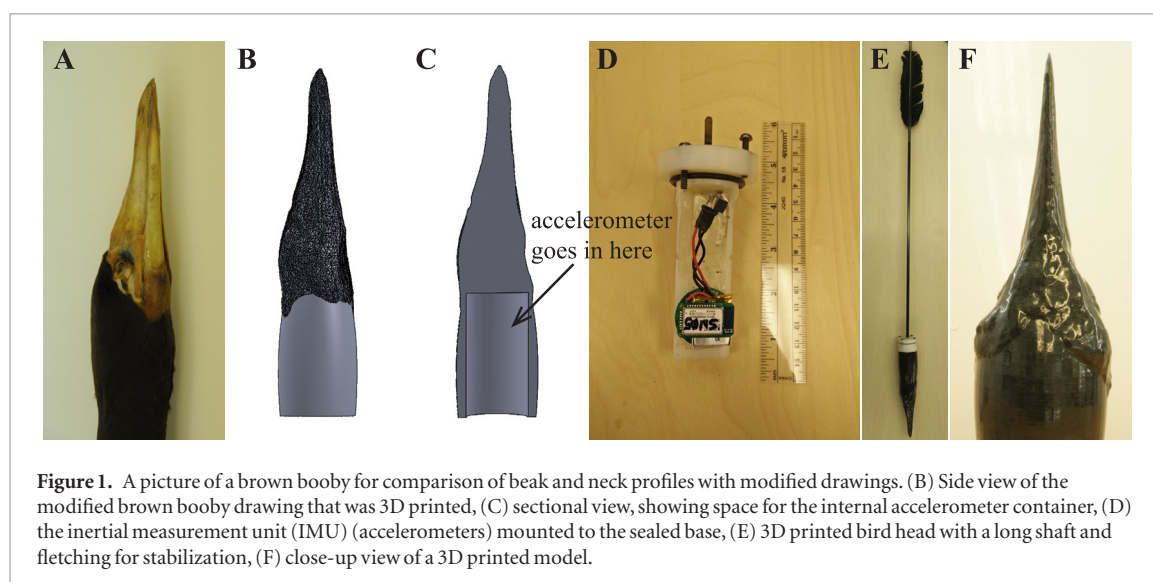


Figure 1. A picture of a brown booby for comparison of beak and neck profiles with modified drawings. (B) Side view of the modified brown booby drawing that was 3D printed, (C) sectional view, showing space for the internal accelerometer container, (D) the inertial measurement unit (IMU) (accelerometers) mounted to the sealed base, (E) 3D printed bird head with a long shaft and fletching for stabilization, (F) close-up view of a 3D printed model.

to find but in general, the average density of a bird is 0.73 g cm^{-3} including lungs and air sacs (Saunders and Manton 1949). Welty (1962) cited 0.9 g cm^{-3} for a duck (without air sacs). The 3D printed bird head models had an average density of 0.88 g cm^{-3} , which can be considered close enough to the actual bird densities.

The final 3D printed model of a northern gannet is shown in figure 1(F). Since the printed bird heads had a heavier rear end which made them prone to rotate during free-fall from the higher speed drops, a long shaft with fletching (i.e. arrow) was attached to their backside for stabilizing purposes, as shown in figure 1(E).

2.2. IMU

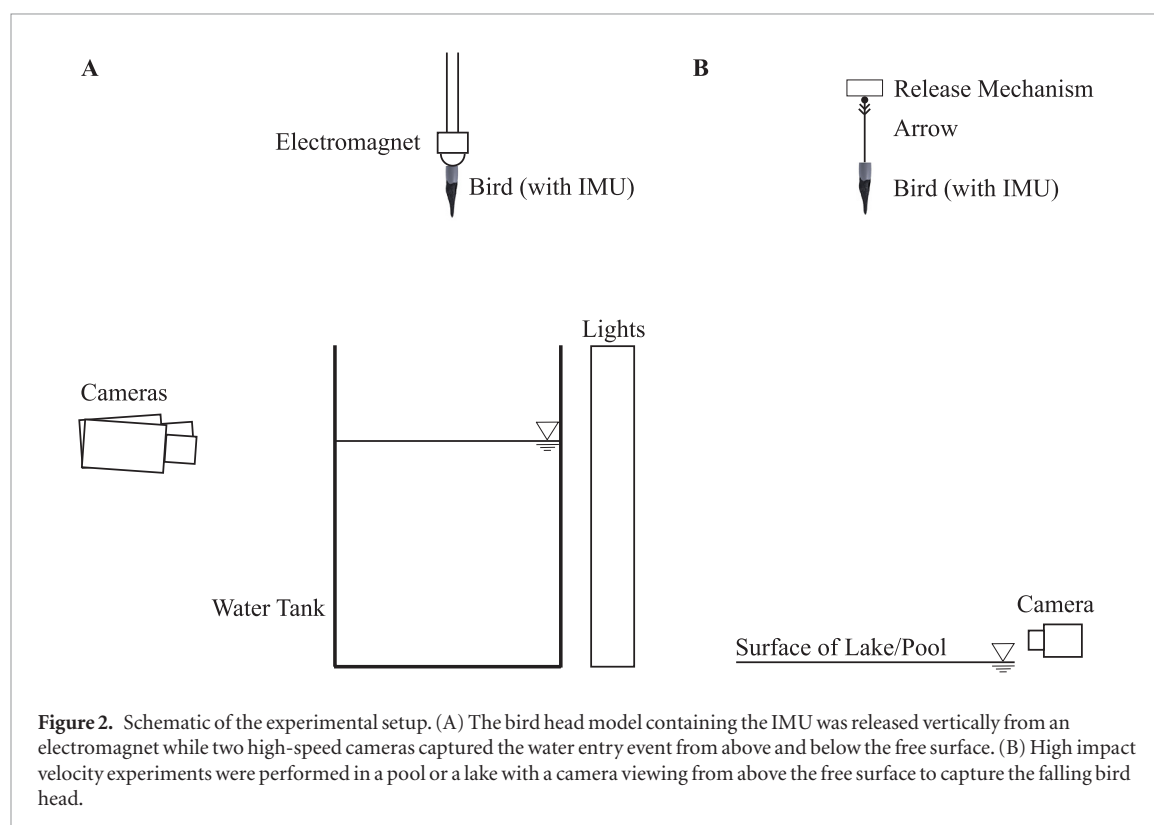
An IMU (InvenSense MPU-9250) consisting of a 3-axis accelerometer, a 3-axis gyroscope and a 3-axis magnetometer was embedded in the bird head models. MPU-9250 is a multi-chip module (MCM) consisting of a gyroscope, an accelerometer and an electronic compass (Asahi Kasei Microdevices AK8963). The

MPU-9250 accelerometer has a maximum range ($\pm 16 \text{ g}$) lower than our expected maximum, hence an additional accelerometer (ST H3LIS331DL) with a maximum range of $\pm 400 \text{ g}$ was added to the unit. Both accelerometers had reported sampling frequencies of 1000 Hz to measure the impact accelerations of the bird head models. The collected data indicated that the accelerometers sampled between 998 Hz and 1002 Hz.

A raw output example of the accelerometers is shown in figures 5(B)–(D). The accelerations are zero while the bird head model is in free fall, impact occurs at $\sim 0.055 \text{ s}$ and the accelerometers increase in value at impact. Although the IMU was capable of measuring rotation angles, it was not used since we were mainly interested in the impact acceleration of these bird head models. The wireless IMU (figure 1(D)) was connected to a computer via Bluetooth[®] and triggered manually or after detecting freefall to start data recording. The unit was placed securely in a waterproof container within the printed birds as shown in figure 1(C).

Table 2. Physical properties of the 3D printed bird heads.

Bird type	Name of bird	Mass (kg)	Beak length (mm)	Neck diameter (mm)
Plunge diving birds				
1	Belted kingfisher (<i>Megaceryle alcyon</i>)	0.375	68.8	41.04
2	Brown booby (<i>Sula leucogaster</i>)	0.292	95.1	48.21
3	Common tern (<i>Sterna hirundo</i>)	0.377	76	29.18
4	Northern gannet (<i>Morus bassanus</i>)	0.452	102.4	68.03
5	Red footed booby (<i>Sula sula</i>)	0.251	69.7	48.91
Dipper				
1	Herring gull (<i>Larus argentatus</i>)	0.452	54.8	68.13
Surface diving birds				
1	Atlantic puffin (<i>Fratercula arctica</i>)	0.349	44.36	41.7
2	Common eider (<i>Somateria mollissima</i>)	0.292	59	52.26
3	Double crested cormorant (<i>Phalacrocorax auritus</i>)	0.248	62.8	40.54
4	Common loon (<i>Gavia immer</i>)	0.349	74.47	58.21
5	Red-breasted merganser (<i>Mergus serrator</i>)	0.263	63	49.84



2.3. Setup

The 3D printed birds were dropped from heights as high as 30 m reaching speeds of up to 23.2 m s^{-1} . Maximum drop heights of only 1 m were permissible in the laboratory where the bird models and embedded accelerometers were dropped vertically from an electromagnet into a glass tank containing water (figure 2(A)). Higher impact velocities were achieved in a 4.7 m deep swimming pool while the highest drop heights were conducted at the Upper Stillwater Dam in Duchesne County, Utah, which had a height of approximately 33 m from the top of the dam to the water surface at the time of the experiment. The 3D printed models and accelerometers in these cases were

lifted to the desired height and released using a remote release mechanism (figure 2(B)). Each bird head model was dropped three times from the same height, except from 30 m where it was dropped just once due to the lack of allowed time and weather conditions at the dam site. Error bars in the figures represent the maximum 95% confidence band using a Student's t -distribution for $n = 3$ cases. The 30 m drop heights have error bands that are not reported since we were only able to drop the bird head models once at that height. Raw data from the IMU for the impact events for two different birds at three different speeds are shown for reference in supplemental information SI figure S1 (stacks.iop.org/BB/14/056013/mmedia).

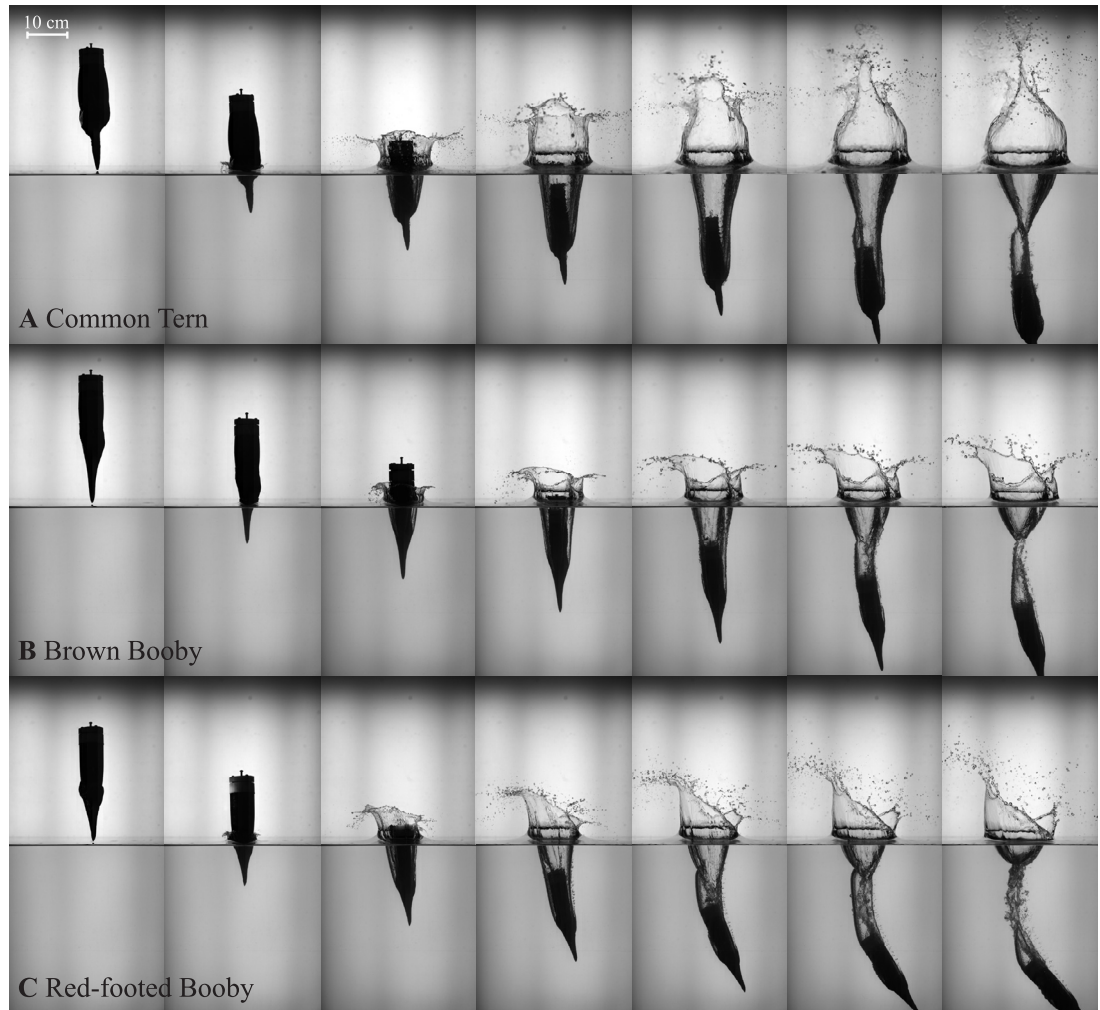


Figure 3. Image sequences showing the water entry of three plunge diving bird heads as marked for an impact velocity of $v = 4.4 \text{ m s}^{-1}$. The time interval between each image is 22 ms. All birds pitch upward after impact in every drop.

At the lowest drop heights in the laboratory, images were captured with two high-speed cameras (Photron SA3, 1000 fps) set orthogonally to check if the bird models entered the water surface vertically (shown in figure 2(B)). At the pool, a single high-speed camera (Photron SA3, 500 fps) was used for imaging below the surface (figure 2(B)). At the pool and the lake, a single 120 fps camera (Sony Alpha 7r) was used above the surface to capture the impact speeds (figure 2(B)). Images were processed using MATLAB[®] to determine the impact velocities for each height.

The impact duration, Δt , used in this paper is defined as the time required to reach from zero to maximum acceleration and is measured in the same manner as by Broglio *et al* (2009). The impact acceleration and the impact duration is used to calculate the impact jerk of the diving birds, where jerk is the time derivative of acceleration ($J = da/dt$) (Eager *et al* 2016). The jerk values are then non-dimensionalized to take into account the differences in masses and neck areas of the birds using the following equation:

$$J^* = \frac{\Delta a}{\Delta t} \cdot \frac{m}{\frac{1}{2}\rho g v A}, \quad (1)$$

where Δa is the change in acceleration during impact, Δt is the impact duration, m is the total mass of the real bird, ρ is the density of water, v is the impact velocity and A is the cross-sectional area of the neck of the bird.

3. Results and discussion

Five plunge diving, one dipper, and five surface diving bird models were dropped into water with impact velocities ranging between $4.4\text{--}23.2 \text{ m s}^{-1}$ (properties are listed in table 2). Image sequences in figures 3 and 4 demonstrate the water entry events of three plunge diving birds (common tern, brown booby and red-footed booby) and three surface diving (Atlantic puffin, common loon and double-crested cormorant), respectively. Air entrainment and cavity formation occurs as the bird head models impact the water surface and travel through the fluid.

The image sequences of the bird head models entering the water were matched with accelerometers at the first moment of impact for all but the highest impact speeds where only accelerometers were used (i.e. not truly synchronized). Figure 5(A) shows an

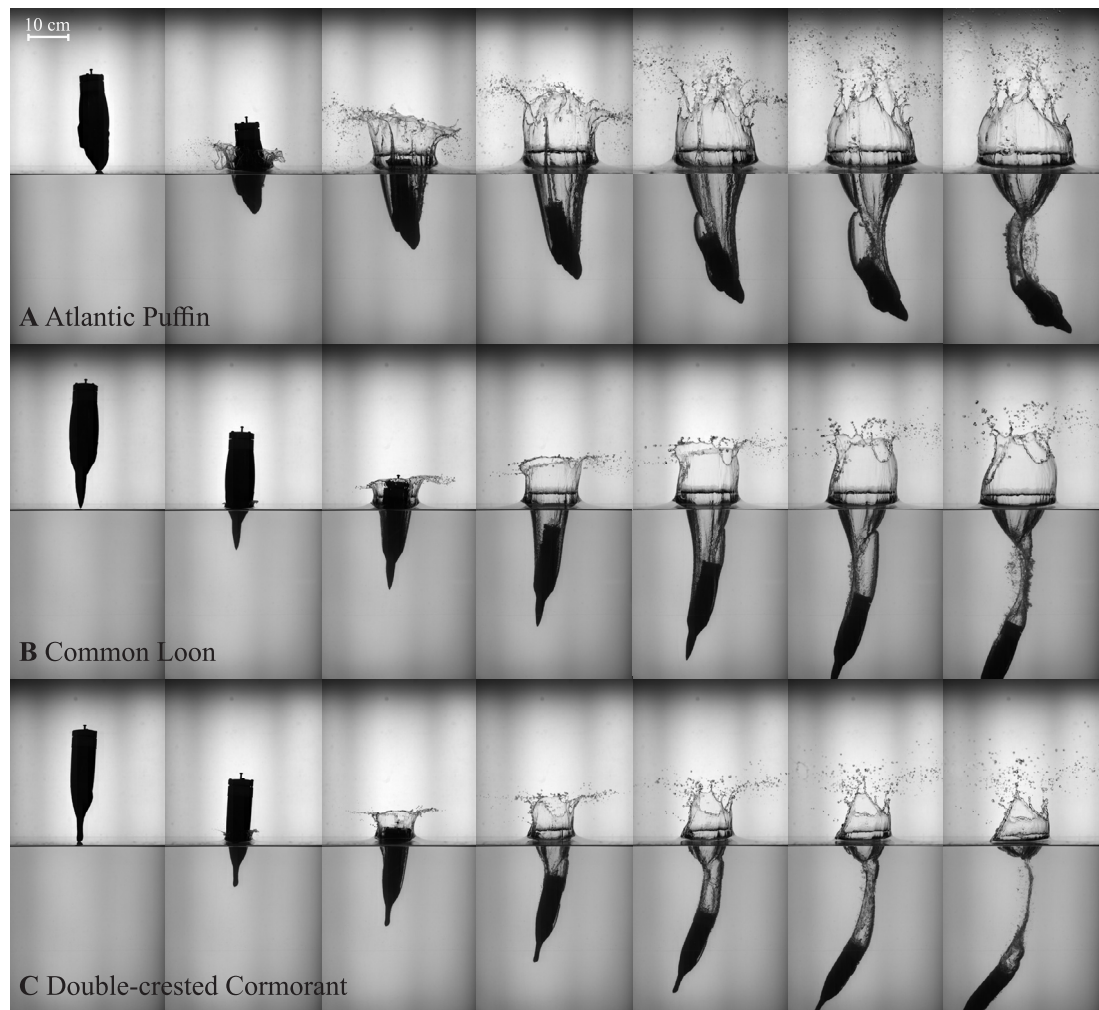


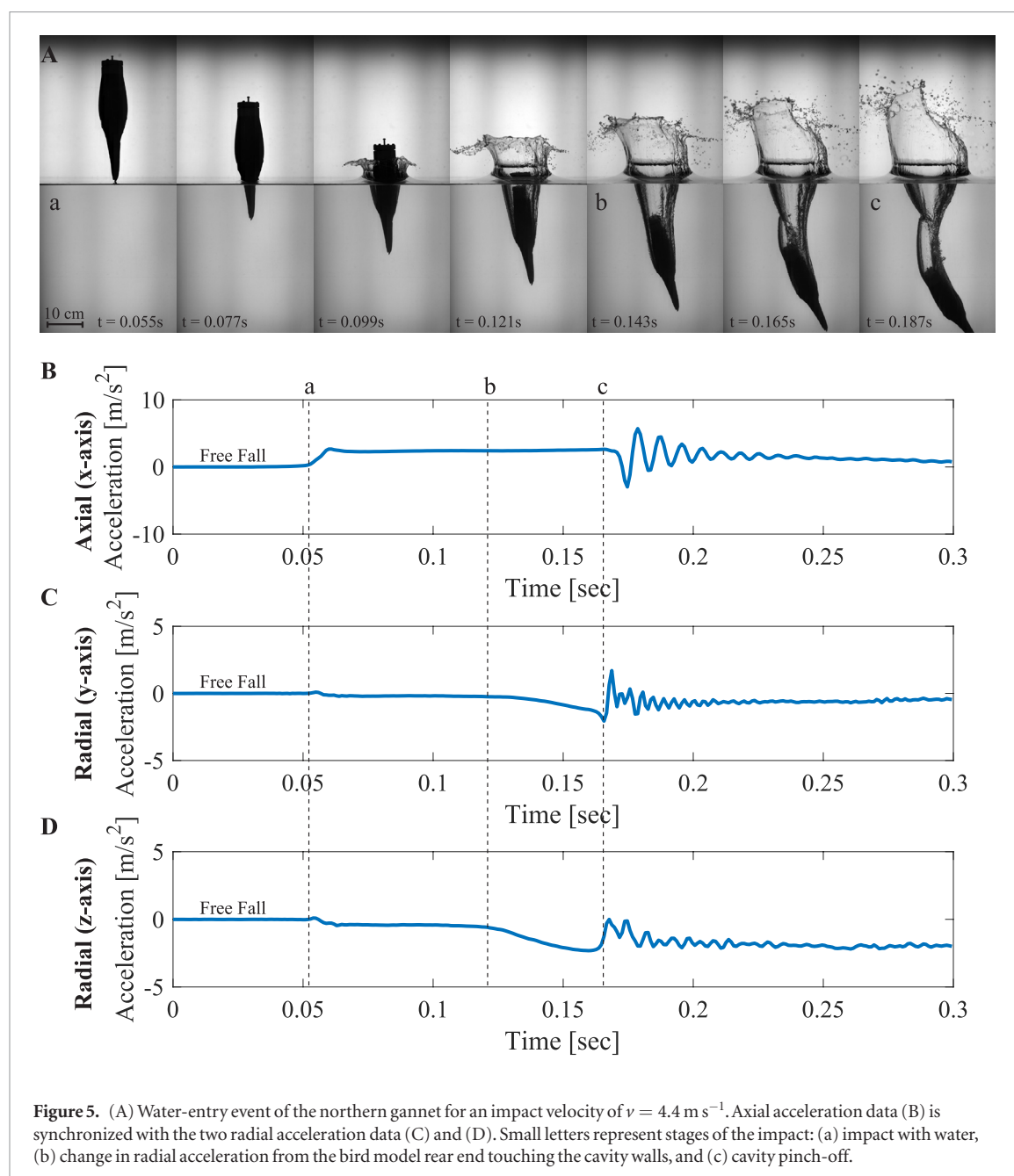
Figure 4. Image sequences showing the water entry of three surface diving bird heads as marked for an impact velocity of $v = 4.4 \text{ m s}^{-1}$. The time interval between each image is 22 ms. The Atlantic puffin pitches upward, whereas the common loon and the double-crested cormorant pitch downward, after impact in every drop.

image-sequence for a plunge diving bird model, the northern gannet, as it enters water (a) at an impact velocity of 4.4 m s^{-1} until the cavity pinches-off (c). Impact acceleration recorded by the accelerometer in figures 5(B)–(D) (a_x , a_y , a_z , respectively) is experienced more prominently in the axial direction as indicated by the sudden increase in acceleration after the free-fall region (a) in figure 5(B), and the lack of any significant acceleration in radial directions in figures 5(C) and (D). Here, axial direction- x refers to the vertical direction along the body of the bird model from head to tail; radial direction- y refers to the direction along the plane of the camera; and the remaining for radial direction- z . This study is focused on the initial phases of impact which starts from line (a) in figure 5(B) to the next immediate peak in acceleration (figure 5(B), $t = 0.055\text{--}0.065 \text{ s}$), where the effects of any rotation from the bird head model are negligible as the model has not had enough time to rotate. The second peak in acceleration appears after the cavity pinches-off (c), causing pressure reverberations typical of cavity collapse (Grumstrup *et al* 2007). The collapse affects the projectile acceleration in all directions with the largest change occurring in the axial direction.

The images also show a pitch down trajectory as the bird travels downward through the water column. This causes the rear end of the bird model to touch the cavity walls (b), disrupting the cavity shape.

Previous literature used cones as an approximation to bird heads (Chang *et al* 2016). Trends in impact acceleration noted by Bodily *et al* (2014) for projectiles with conical and ogive noses resemble the accelerometer results (figure 5) obtained for diving bird models in this study. However, comparing maximum drag coefficients obtained in the present study to those of cones from experiments by Baldwin (1971) reveals that the bird heads experience significantly larger drag coefficients (i.e. forces) than cones and that they do not seem to have a significantly increasing drag with increasing angle (see SI figure S2). The difference arises from bird heads having varying beak angle values in the azimuthal plane, unlike cones which are uniformly shaped objects. Hence, using exact 3D printed replicas of bird heads instead of approximating them as cones provides more accurate results.

Most bird beaks have two distinct angles, one of which can be measured from the side view, and the other from the top view. In this study, we use a ratio



of these two beak angles, called the beak angle ratio defined as the top angle divided by the side angle, presented in figure 6(A), where the beak angle ratio ranges from 0 to 1, with 1 being the highest possible ratio. The beak angle was measured from a point where a line drawn would maximize the coincidence with the contour of the beak. This provided results that matched closely with Chang *et al* (2016) angle data. High beak angle ratios (e.g. red-footed booby) result from both these angles being in close proximity while low beak angle ratios (e.g. Atlantic puffin) occur when the difference is greater. Measurement of the top and side angles is shown in figures 6(B) and (C). The dotted line (at beak angle ratio ~ 0.54 , figure 6(A)) separates birds based on their beak angle ratios: plunge diving birds fall above the line (0.565–0.822), while the dipper (0.52) and surface diving birds (0.125–0.428) lie below the line with one exception, the merganser. It is a sur-

face diver with a beak characterized by a round tip and thus a high beak angle ratio of 1 (see SI figure S5).

A measure of the impact force experienced by the 3D printed bird heads can be obtained by comparing impact accelerations (a) during water-entry. The impact accelerations of all bird heads with impact velocities ranging between $4.4\text{--}23.2 \text{ m s}^{-1}$ are shown in figure 7. The maximum uncertainty was calculated for all cases based on a 95% confidence interval with a Student's *t*-distribution. This was found to be $\pm 25.5 \text{ m s}^{-2}$ for plunge diving and $\pm 27.2 \text{ m s}^{-2}$ for surface diving birds. We define the impact acceleration as the first peak in acceleration directly after impacting the water surface (e.g. $t \sim 0.05 \text{ s}$ or 'a' in figure 5(B)). Although accelerations in the radial direction are much lower than those in the axial direction, the overall impact acceleration considered is a measure of accelerations in all three directions of the accel-

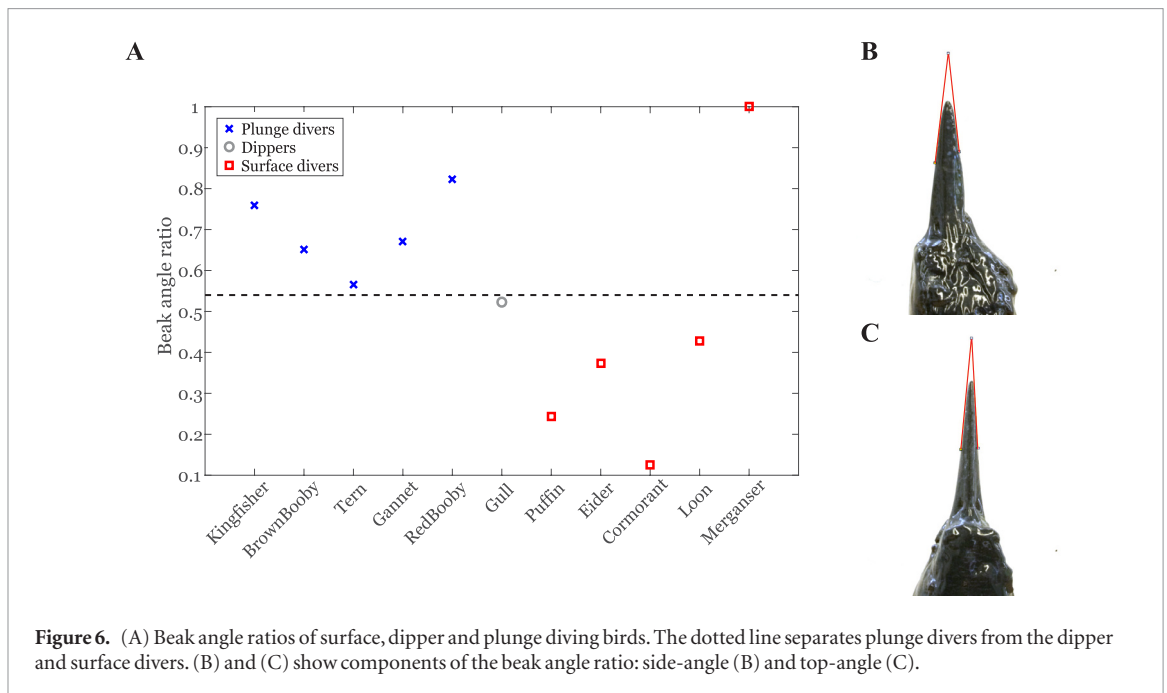


Figure 6. (A) Beak angle ratios of surface, dipper and plunge diving birds. The dotted line separates plunge divers from the dipper and surface divers. (B) and (C) show components of the beak angle ratio: side-angle (B) and top-angle (C).

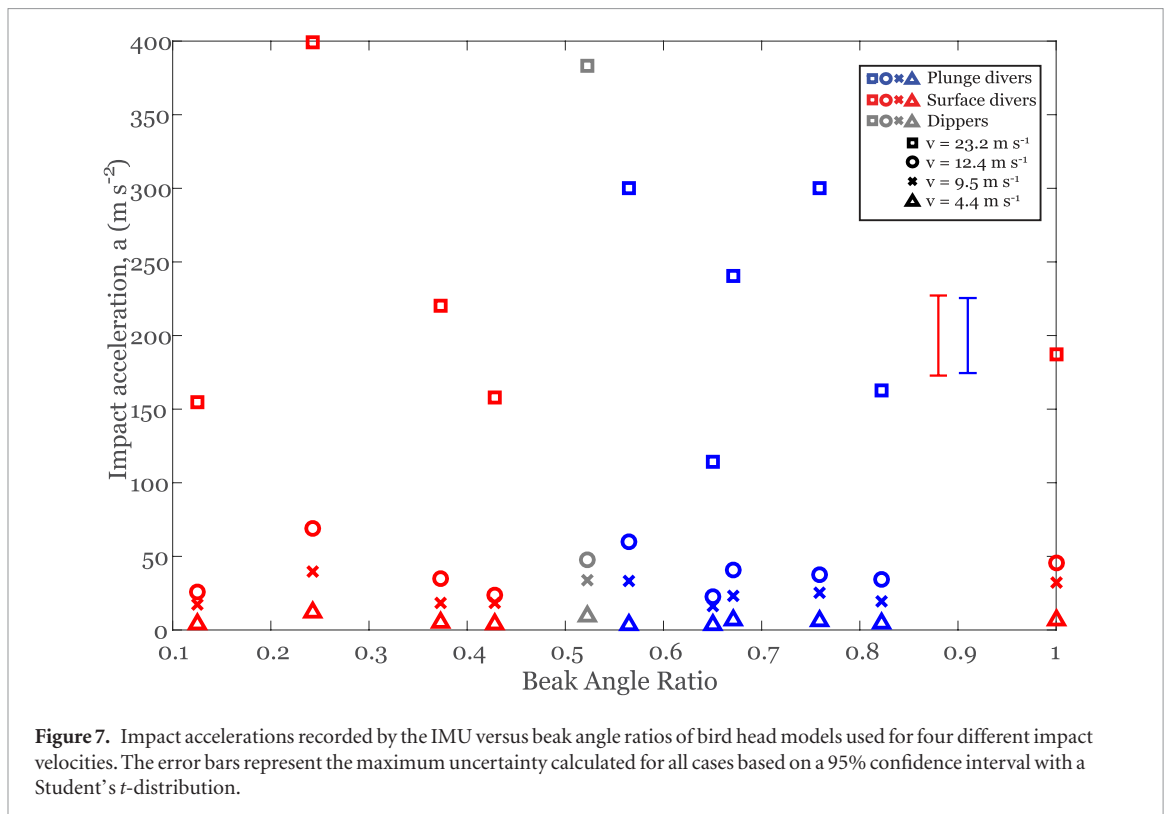
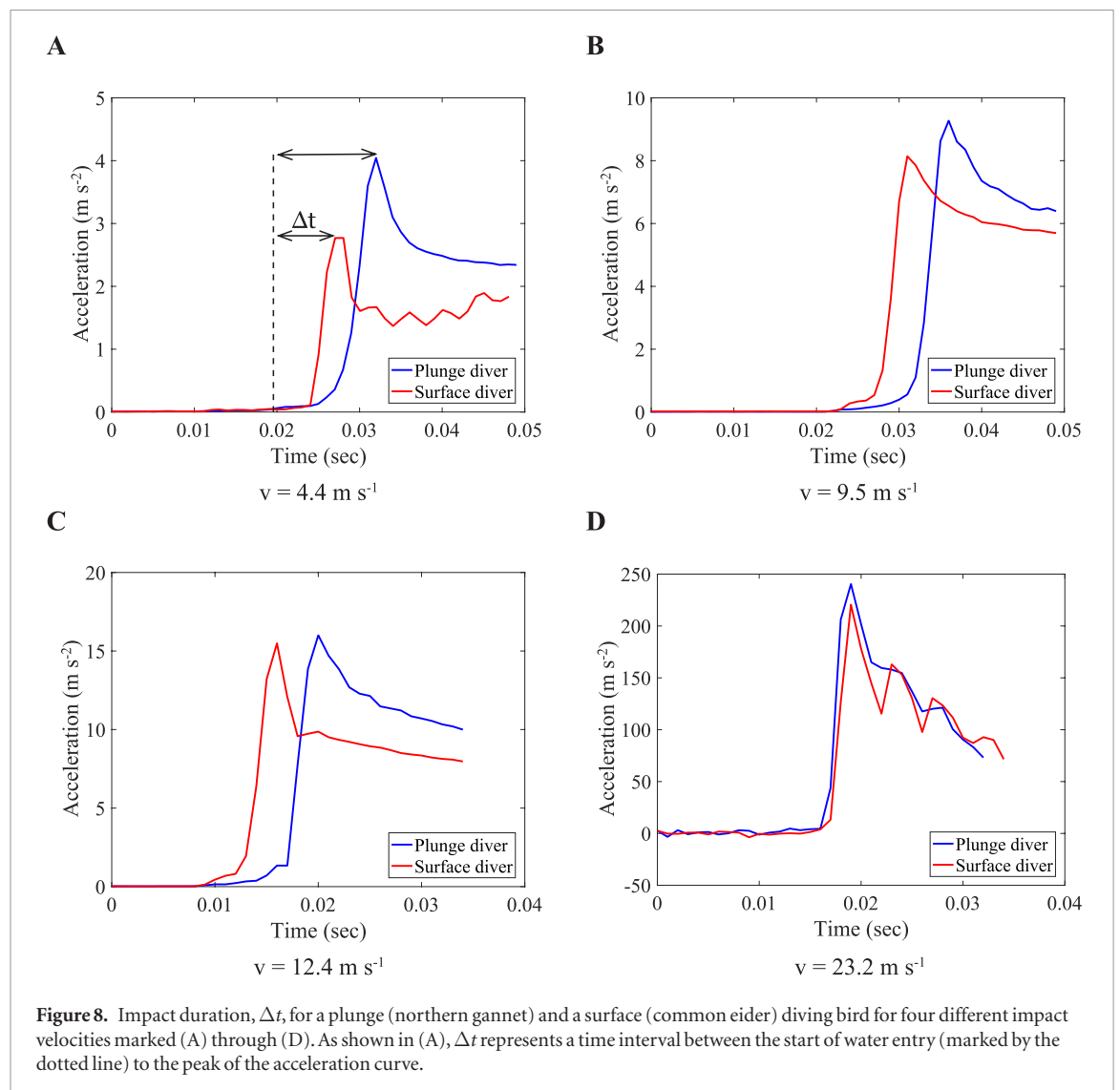


Figure 7. Impact accelerations recorded by the IMU versus beak angle ratios of bird head models used for four different impact velocities. The error bars represent the maximum uncertainty calculated for all cases based on a 95% confidence interval with a Student's *t*-distribution.

ometer axes (i.e. $a = \sqrt{a_x^2 + a_y^2 + a_z^2}$). Figure 7 does not appear to show any obvious trend separating surface diving, dipper or plunge diving birds. Some plunge divers (114.3–300.1 m s⁻²) record higher impact accelerations than surface divers (154.4–399.2 m s⁻²), while others record lower, and vice versa. The same can be said about the impact forces when a Force, *F* versus beak angle ratio plot is observed (SI figure S3), where $F = ma$.

In fact, our data indicates that surface divers could safely dive from heights as high as plunge divers when

using the methodology of Chang *et al* (2016). Experiments performed by Chang *et al* using cones and elastic beams as bird head and neck replicas, respectively, identified unstable (bent neck) and stable regimes (not bent). Their analysis estimated that northern gannets and brown boobies dive in a stable regime, capable of diving with impact velocities of up to 24 m s⁻¹ without incurring any injury. Herein, all of the bird models we tested including surface divers are found to dive in the stable regime at the highest impact velocities as calculated and shown in SI figure S4. This data implies that surface divers are capable of diving at high speeds but



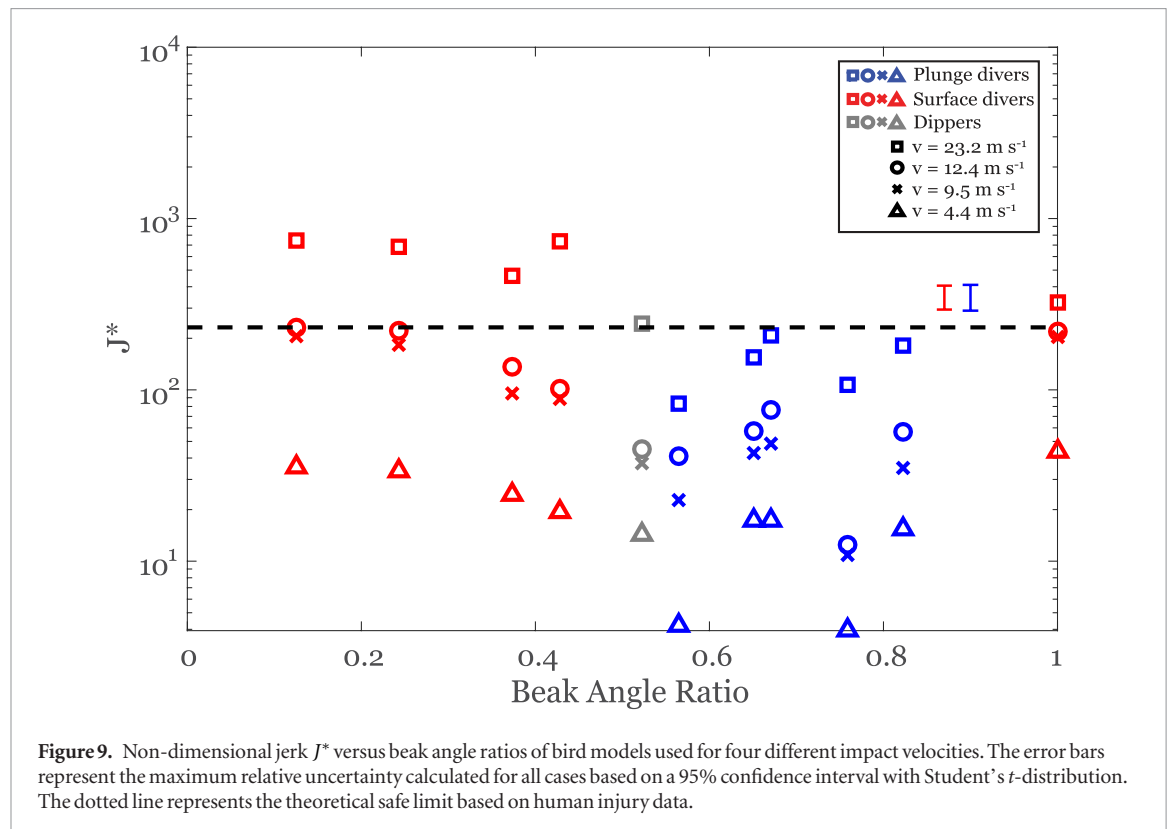
yet they do not. Is there a physical limit to plunge dive safely or is the dive speed regulated to moderate dive depth and the ability to capture fish?

Although we cannot answer whether or not these are behavioral traits, we can explore another important property considered in impact events like car accidents. The destructive effect of sudden changes in motion is called ‘jerk’ and is defined as the rate of change of acceleration, where large values of jerk are considered dangerous or destructive (Eager *et al* 2016). The bird models experience a very rapid change in acceleration upon water-entry similar to a human in a car accident. Herein, the jerk is based on the entire duration during which the impact event occurs (as shown in figure 5) starting from zero acceleration to maximum. An instantaneous jerk using the slope of the steepest part of the data from the accelerometer was not used because the event is so fast it is possible that the accelerometers did not capture the true slope. Instead, the jerk was calculated using the time from the beginning of the slope change to the maximum.

Analysis of all individual accelerometer data recorded reveals the impact duration to be longer for plunge divers and shorter for surface divers impact-

ing at identical velocities even though the maximum accelerations are similar. Figure 8 shows the impact duration, Δt , at four different impact velocities for a plunge diver (northern gannet) and a surface diver (common eider). All impact durations were measured similarly as shown in figure 8(A), starting from an increase in acceleration from zero to maximum. For accuracy, the impact durations were directly measured from the accelerometer data. The plots in figure 8 are a small part of the whole acceleration data as in figure 5, focusing on the impact region.

The masses and neck areas of each bird are different, so non-dimensionalizing the jerk value (J^*) is important for the analysis and is defined in equation (1). The J^* values for all birds tested in this study are shown in figure 9. The dotted line represents a theoretical safe limit calculated from equation (1) based on data obtained from human injury experiments, due to the lack of literature on the safe limits of J^* for bird water entry impact. According to Hill (1950), the inherent strength of a contracting voluntary muscle fiber is roughly constant and is independent of the size of the animal. Additionally, the maximum stress that a mammalian muscle can exert is found to be 0.35 MPa (Mad-



den *et al* 2004) and that of a bird muscle is found to be 0.30 MPa (Pennycuik 1996), which support Hill's conclusion. Thus, considering that birds and humans have similar muscle strength, we non-dimensionalize information from human water impact injury studies to calculate the safe limit for J^* of birds. Of the two critical impact velocities reported for human survival in free fall impacts onto water, we use $v = 30.5 \text{ m s}^{-1}$ (Snyder 1965, Kumar and Norfleet 1992). Similarly, some experiments on athletes have been conducted to determine the critical impact acceleration of 765.2 m s^{-2} (Withnall *et al* 2005) and duration of 15 ms (Pellman *et al* 2003) that could result in a concussion.

According to this limiting non-dimensional jerk, any value that falls below the dotted line in figure 9 is considered safe and anything above is unsafe. Surface and plunge divers have similar J^* values for low impact speeds but distinctions arise as impact velocity increases. The dipper (Herring gull) is found to have a J^* value similar to those of plunge divers. This is expected, as Herring gulls are often observed to make plunge dives (Verbeek 1977, Sibly and McCleery 1983) and have beak angle ratios close to plunge divers. While surface diving birds appear divided by the line, all plunge diving birds and the dipper fall within the safe region even for the highest impact velocities tested. Surface divers diving at lower impact velocities are found to be in or near the safe region, still being close to the limit. However, none of the surface divers fall in the safe region when impacting at 23.2 m s^{-1} . The proposed safety limit can explain why surface divers do not dive from high heights and indicates that J^* could be a deciding factor in determining

whether a bird can dive or not. Larger J^* for surface divers, in general, can be attributed to the differences in their beak shapes. Beak shape in birds has been associated with prey type (Grant and Grant 1993, Bright *et al* 2016), although allometry of the skull can influence the size of the beak (Bright *et al* 2016). The mechanics and functional morphology of avian structures remains poorly understood (Rubega 2000). This includes the relationship between the fluid dynamics and feeding. The black skimmer (*Rhyncops nigra*) has a lower beak morphology with a tapered leading edge to reduce drag as it moves along the air–water interface to catch fish (Withers and Timko 1977). The spoonbill (*Platalea leucordia*) sweeps its spatulate, flattened bill through the water to shed vortices creating hydrodynamic suction, which move prey to the mouth (Weihs and Katzir 1994). Chang *et al* (2016) examined the hydrodynamic influence of the beak during plunge diving on neck stabilization. We observe that surface diving birds generally have blunt beak tips with rapidly varying cross-sections whereas plunge divers have sharply pointed beak tips for better water entry characterized by a gradual increase in cross-section as illustrated in figures 6 and SI S5. The analysis indicates that an ideal plunge diving bird should have a high beak angle ratio with a sharply pointed beak tip and a gradual increase in cross-section towards the head. Perhaps the beak angle is not unique to diving birds, instead it may be a small prerequisite for efficient plunge diving rather than the only requirement. For instance, a non-diving bird with a large beak angle ratio would have low J^* values in the tests performed here.

4. Conclusions

This study presents the initial water-entry dynamics of diving birds to understand why plunge divers can dive into water at high speeds but surface divers do not based on the morphology of the beak and head. An embedded IMU is used to measure the impact accelerations of eleven 3D-printed bird head models (five plunge diving, one dipper, and five surface diving birds) for impact velocities ranging between 4.4–23.2 m s⁻¹. Surface divers are noted to have smaller beak angle ratios (0.125–0.428) than plunge divers (0.565–0.822), with the exception of the merganser (1.0) having a nearly symmetric beak tip. Impact accelerations experienced for the highest impact velocity by plunge divers (114.3–300.1 m s⁻²), dipper (383 m s⁻²) and surface divers (154.4–399.2 m s⁻²) are not distinguishable. However, the jerk values of surface and plunge divers are quite different at the highest velocities. We introduce a non-dimensional jerk, J^* , having a safe limit based on human injury and survival data. At the highest impact speeds tested, surface divers are found to be associated with J^* values exceeding the safe limit while all plunge divers and the dipper are not. Thus, the non-dimensional jerk provides a potential measurement, among other factors, to explain why surface diving birds avoid plunge diving acrobatic techniques.

Acknowledgments

We wish to express our appreciation to the Delaware Museum of Natural History and Jean Woods (Curator of Birds) for access to their ornithological collection. We thank Danielle Adams, William Gough, and Kelsey Tennett for assistance with 3D scanning. The 3D scanning system was purchased with funds from the Office of Naval Research (N000141512667). We also thank Troy Ovard for providing access to the Upper Stillwater Dam.

ORCID iDs

Tadd T Truscott  <https://orcid.org/0000-0003-1613-6052>

References

- Adams N J and Walter C B 1993 Maximum diving depths of cape gannets *Condor* **95** 734–6
- Alderfer J 2008 *National Geographic Complete Birds of North America* National Geographic (Washington DC: National Geographic) p 362
- Baldwin J L 1971 Vertical water entry of cones *Technical Report AD0723821* Naval Ordnance Lab, White Oak, MD.
- Bodily K G, Carlson S J and Truscott T T 2014 The water entry of slender axisymmetric bodies *Phys. Fluids* **26** 072108
- Brierley A S and Fernandes P J 2001 Diving depths of northern gannets: acoustic observations of *Sula bassana* from an autonomous underwater vehicle *Auk* **118** 529–34
- Bright J A, Marugán-Lobón J, Cobb S N and Rayfield E J 2016 The shapes of bird beaks are highly controlled by nondietary factors *Proc. Natl Acad. Sci.* **113** 5352–7
- Broglio S P, Sosnoff J J, Shin S, He X, Alcaraz C and Zimmerman J 2009 Head impacts during high school football: a biomechanical assessment *J. Athl. Train.* **44** 342–9
- Castro P and Huber M E 2008 *Marine Biology* 7th edn (Boston, MA: McGraw Hill)
- Chang B, Croson M, Straker L, Gart S, Dove C, Gerwin J and Jung S 2016 How seabirds plunge-dive without injury *Proc. Natl Acad. Sci.* **113** 12006–11
- Eager D, Pendrill A M and Reistad N 2016 Beyond velocity and acceleration: jerk, snap and higher derivatives *Eur. J. Phys.* **37** 065008
- Eroshin V A, Romanenkov N I, Serebryakov I V and Yakimov Y L 1980 Hydrodynamic forces produced when blunt bodies strike the surface of a compressible fluid *Fluid Dynamics* **15** 829–35
- Garthe S, Benvenuti S and Montevecchi W A 2000 Pursuit plunging by northern gannets (*Sula bassana*) feeding on capelin (*Mallotus villosus*) *Proc. R. Soc. B* **267** 1717–22
- Grant B R and Grant P R 1993 Evolution of Darwin's finches caused by a rare climatic event *Proc. R. Soc. B* **251** 111–7
- Grumstrup T, Keller J B and Belmonte A 2007 Cavity ripples observed during the impact of solid objects into liquids *Phys. Rev. Lett.* **99** 114502
- Guillemette M, Ydenberg R C and Himmelman J H 1992 The role of energy intake rate in prey and habitat selection of common eiders *Somateria mollissima* in winter: a risk-sensitive interpretation *J. Animal Ecol.* **61** 599–610
- Hill A V 1950 The dimensions of animals and their muscular dynamics *Sci. Prog.* **38** 209–30
- Korobkin A A and Pukhnachov V V 1988 Initial stage of water impact *Annu. Rev. Fluid Mech.* **20** 159–85
- Kumar K V and Norfleet W T 1992 Issues on human acceleration tolerance after long-duration space flights *Technical Memorandum* 104753 NASA
- Le Corre M 1997 Diving depths of two tropical Pelecaniformes: the red-tailed tropicbird and the red-footed booby *Condor* **99** 1004–7
- Lee D N and Reddish P E 1981 Plummeting gannets: a paradigm of ecological optics *Nature* **293** 293–4
- Liang J, Yang X, Wang T, Yao G and Zhao W 2013 Design and experiment of a bionic gannet for plunge-diving *J. Bionic Eng.* **10** 282–91
- Machovsky-Capuska G E, Dwyer S L, Alley M R, Stockin K A and Raubenheimer D 2011b Evidence for fatal collisions and kleptoparasitism while plunge diving in Gannets *Ibis* **153** 631–5
- Machovsky-Capuska G E, Vaughn R L, Würsig B, Katzir G and Raubenheimer D 2011a Dive strategies and foraging effort in the Australasian Gannet *Morus serrator* revealed by underwater videography *Mar. Ecol. Prog. Ser.* **442** 255–61
- Madden J D, Vandesteeg N A, Anquetil P A, Madden P G, Takshi A, Pytel R Z, Lafontaine S R, Wieringa P A and Hunter I W 2004 Artificial muscle technology: physical principles and naval prospects *IEEE J. Ocean. Eng.* **29** 706–28
- May A 1975 Water entry and the cavity-running behavior of missiles *Technical Report* 20910 Nav. Surf. Weapons Cent., White Oak Lab., MD
- Moghisi M and Squire P T 1981 An experimental investigation of the initial force of impact on a sphere striking a liquid surface *J. Fluid Mech.* **108** 133–46
- Pellman E J, Viano D C, Tucker A M, Casson I R and Waeckerle J F 2003 Concussion in professional football: reconstruction of game impacts and injuries *Neurosurgery* **53** 799–814
- Pennycuik C J 1996 Stress and strain in the flight muscles as constraints on the evolution of flying animals *J. Biomech.* **29** 577–81
- Perrins C 2003 *The New Encyclopedia of Birds* (Oxford: Oxford University Press)
- Ropert-Coudert Y, Gremillet D, Ryan P, Kato A, Naito Y and Le Maho Y 2004 Between air and water: the plunge dive of the cape gannet *Morus capensis Ibis* **146** 281–90

- Rubega M 2000 Feeding in birds: approaches and opportunities *Feeding: Form, Function, and Evolution in Tetrapod Vertebrates* ed K Schwenk (San Diego, CA: Academic) pp 395–408
- Saunders J T and Manton S M 1949 *Manual of Practical Vertebrate Morphology* (Oxford: Oxford University Press)
- Shiffman M and Spencer D C 1945 The force of impact on a sphere striking a water surface *AMP-42.2R-AMG-NYU* No. 133 New York University
- Sibly R and McCleery R 1983 The distribution between feeding sites of herring gulls breeding at Walney Island UK *J. Animal Ecol.* **52** 51–8
- Snyder R G 1965 *Survival of High-Velocity Free-Falls in Water* (Oklahoma: Civil Aeromedical Research Institute) p AM 65-12
- Truscott T T, Epps B P and Belden J 2014 Water entry of projectiles *Annu. Rev. Fluid Mech.* **46** 355–78
- Verbeek N A M 1977 Comparative feeding behavior of immature and adult herring gulls *Wilson Bull.* **89** 415–21
- Wang T M, Yang X B, Liang J H, Yao G C and Zhao W D 2013 CFD based investigation on the impact acceleration when a gannet impacts with water during plunge diving *Bioinspir. Biomim.* **8** 036006
- Weihls D and Katzir G 1994 Bill sweeping in the spoonbill, *Platalea leucordia*: evidence for a hydrodynamic function *Animal Behav.* **47** 649–54
- Weisler W, Stewart W, Anderson M B, Peters K J, Gopalathnam A and Bryant M 2017 Testing and characterization of a fixed wing cross-domain unmanned vehicle operating in aerial and underwater environments *IEEE J. Ocean. Eng.* **99** 1–14
- Welty J C 1962 *The Life of Birds* (Philadelphia, PA: W B Saunders and Co.)
- Withers P C and Timko P L 1977 The significance of ground effect to the aerodynamic cost of flight and energetics of the black skimmer (*Rhyncops nigra*) *J. Exp. Biol.* **70** 13–26
- Withnall C, Shewchenko N, Gittens R and Dvorak J 2005 Biomechanical investigation of head impacts in football *Br. J. Sports Med.* **39** i49–57
- Wu Y, Li L, Su X and Gao B 2019 Dynamics modeling and trajectory optimization for unmanned aerial-aquatic vehicle diving into the water *Aerosp. Sci. Technol.* **89** 220–9
- Yang X, Wang T, Liang J, Yao G and Liu M 2015 Survey on the novel hybrid aquatic–aerial amphibious aircraft: aquatic unmanned aerial vehicle (AquaUAV) *Prog. Aerosp. Sci.* **74** 131–51